Oncogene (2002) 21, 2662–2669

www.nature.com/onc

Anti-neovascular therapy using novel peptides homing to angiogenic vessels

Naoto Oku*,[1], Tomohiro Asai[1], Koh Watanabe[1], Koichi Kuromi[1], Mayumi Nagatsuka[1], Kohta Kurohane[1], Hironori Kikkawa[1], Koichi Ogino[2], Michinori Tanaka[2], Dai Ishikawa[2], Hideo Tsukada[3], Masanobu Momose[4], Jun Nakayama[4] and Takao Taki[2]

[1]*Department of Medical Biochemistry, School of Pharmaceutical Sciences, University of Shizuoka, 52-1 Yada, Shizuoka 422-8526, Japan;* [2]*Molecular Medical Science Institute, Otsuka Pharmaceutical Co., Ltd., 463-10 Kagasuno, Kawauchi-cho, Tokushima 771-0192, Japan;* [3]*Hamamatsu Photonics K.K., 5000 Hirakuchi, Hamakita, Shizuoka 434-0041, Japan;* [4]*Department of Laboratory Medicine and Central Clinical Laboratories, Shinshu University Hospital, 3-1-1 Asahi, Matsumoto, Nagano 390-8621, Japan*

Cancer chemotherapy targeted to angiogenic vessels is expected to cause indirect tumor regression through the damage of the neovasculature without the induction of drug resistance. To develop a tool for neovasculature-specific drug delivery, we isolated novel peptides homing to angiogenic vessels formed by a dorsal air sac method from a phage-displayed peptide library. Three distinct phage clones that markedly accumulated in murine tumor xenografts presented PRPGAPLAGSWPGTS-, DRWRPALPVVLFPLH- or ASSSYPLIHWRPWAR-peptide respectively. After the determination of the epitope sequences of these peptides, we modified liposomes with epitope penta-peptides. Liposome modified with APRPG-peptide showed high accumulation in murine tumor xenografts, and APRPG-modified liposome encapsulating adriamycin effectively suppressed experimental tumor growth. Finally, specific binding of APRPG-modified liposome to human umbilical endothelial cells, and that of PRP-containing peptide to angiogenic vessels in human tumors, i.e., islet cell tumor and glioblastoma, were demonstrated. The present study indicates the usefulness of APRPG-peptide as a tool for anti-neovascular therapy, a novel modality of cancer treatment.
Oncogene (2002) **21,** 2662–2669. DOI: 10.1038/sj/onc/1205347

Keywords: anti-neovascular therapy; phage-displayed peptide library; liposome; PRP

Introduction

After the discovery of angiostatin (O'Reilly *et al*., 1996), tumor dormancy therapy became a possible modality; and many attempts have been made to develop angiogenesis inhibitors. Anti-angiogenic drugs are thought to be free of severe side effects that are usually seen with cytotoxic anticancer drugs (Boehm *et al*., 1997). Furthermore, anti-angiogenic therapy is thought not only to eradicate primary tumor tissues, but also suppress tumor metastases (Skobe *et al*., 1997). Besides anti-angiogenic therapy, anti-neovascular therapy, i.e. indirect lethal damage of tumor cells through the damage of newly formed blood vessels, is also promising. Cytotoxic anticancer drugs cause damage to growing neovascular endothelial cells as well as tumor cells. Although tumor cells often acquire drug-resistance, neovascular endothelial cells would not be expected to acquire drug-resistance. Recently, it was suggested that cancer chemotherapy using anti-neovascular scheduling induced endothelial cell apoptosis prior to tumor cell apoptosis in tumor tissues and eradicated the tumor cells (Browder *et al*., 2000). In addition, anti-neovascular-scheduled chemotherapy combined with angiogenesis inhibitor eradicated even the drug-resistant tumor cells (Browder *et al*., 2000).

Furthermore, tumor angiogenic vasculature is thought to be an ideal target site for a drug delivery system (Brown and Giaccia, 1998; Langer, 1998; Zetter, 1997). Newly formed blood vessels have the characteristics of high permeability induced by vascular endothelial growth factor (VEGF)/vascular permeability factor (VPF), and macromolecules such as liposomes are known to passively accumulate in tumor tissues as a reflection of the feature (Asai *et al*., 1998; Oku, 1999a). On the other hand, angiogenesis consists of a complex process involving the recruitment of endothelial progenitor cells (Asahara *et al*., 1997, 1999; Ito *et al*., 1999), as well as proliferation, migration and capillary formation by activated-endothelial cells. Since several growth factors, matrix metalloproteases, and adhesion molecules are involved in these steps, activated-endothelial cells express several specific marker molecules that are not or little expressed on preexisting vessels (St Croix *et al*., 2000). These distinct marker molecules may provide active targeting guides for anti-angiogenic therapy and for anti-neovascular therapy.

In the present study, we isolated peptides specific for tumor angiogenic vasculature using a phage-displayed peptide library (Scott and Smith, 1990). In general, biopanning of a phage-displayed peptide library is performed *in vitro*: The desired short peptide-expressing phages are isolated by their ability to bind to

*Correspondence: N Oku; E-mail: oku@u-shizuoka-ken.ac.jp.
Received 27 November 2001; revised 12 January 2002; accepted 18 January 2002

specific antibodies (Ishikawa *et al*., 1998; Takikawa *et al*., 2000), proteins (Gho *et al*., 1997; Healy *et al*., 1995; Koivunen *et al*., 1993), or glycoconjugates (Martens *et al*., 1995). On the other hand, Pasqualini and Ruoslahti (1996) developed a strategy of *in vivo* biopanning: The phage-displayed peptide library is directly injected into the bloodstream of animals to isolate specific peptide-expressing phage clones homing to the desired organ. By this method, they isolated RGD-containing peptide-expressing phage clones after injection of the phage-displayed peptide library into tumor-bearing mice (Arap *et al*., 1998; Pasqualini *et al*., 1997). In here, we injected a phage-displayed peptide library into angiogenesis model mice prepared by the dorsal air sac (DAS) method (Kurohane *et al*., 2001) instead of tumor-bearing mice, and isolated phage clones specifically accumulated in angiogenic site. The advantage of this method is that the selected phages have the ability to bind only to angiogenic vessels, not to tumor cells. In fact, the amino acid sequences of the phage clones thus obtained were different from any reported sequences obtained by *in vivo* biopanning with tumor-bearing mice. The selected phage clones had high affinity to murine angiogenic vessels. Then, we apply the peptide as a drug delivery system to the neovasculature. Our results demonstrated that anti-neovascular therapy using liposome modified with the novel peptide markedly suppressed tumor growth possibly through cytotoxic effect of the encapsulated drug against angiogenic endothelial cells. Finally, confocal microscopic observation and histochemical staining demonstrated the applicability of the peptide obtained here to human.

Results

Isolation of the peptides homing to angiogenic vessels

We performed biopanning of the phage-displayed peptide library in DAS model mice in a total of five rounds. At the fifth round of biopanning, the recovery rate of the phage (recovered phage titer to input phage titer) increased about 1000-fold over that of the first round (data not shown), suggesting that selection of high-affinity phage clones capable of accumulating in the angiogenic site was successful. After cloning the selected phages, we performed sequencing of the peptides expressed on 13 selected phage clones. Five out of thirteen clones showed the same sequence, and some amino acid sequences of the other eight clones showed several partial homologies (Table 1). To select phage clones having high affinity for tumor angiogenic vasculature, we injected each phage clone intravenously into tumor-bearing mice and examined their capability to accumulate in the tumor. In this experiment, we used implanted tumors instead of the DAS model, since affinity-selected phage clones against angiogenic vasculature would be expected to accumulate in the tumor tissue. In case of injection into B16BL6 melanoma-bearing mice, PRPGAPLAGSWPGTS, DRWRPALPVVLFPLH, and ASSSYPLIHWRPWAR peptide-presented phage clones accumulated in the tumor more than 20-fold compared with the accumulation of the original phage library (Table 1). These clones also accumulated in Meth A sarcoma xenografts (Table 1). To confirm the capability of the synthetic peptides to accumulate in the tumor, we co-injected selected phage clones and corresponding synthetic pentadecapeptides into B16BL6 melanoma-bearing mice. Tumor accumulation of each phage clone was suppressed in the presence of the corresponding 15 mer peptide, although a random 15 mer peptide, GLDLLGDVRIPVVRR, did not affect the phage accumulation (Table 2).

APRPG-modified liposome accumulates in murine tumor xenografts

Next, we determined the epitope sequences of the peptides. DRWRPALPVVLFPLH and ASSSY-PLIHWRPWAR, which contain the common sequence of WRP, showed cross-reactivity (Table 2). In view of these findings, we synthesized fragment peptides focusing on the WRP sequence, and examined the inhibitory effect of these peptides against tumor accumulation of the corresponding phage clones. The fragment peptides containing WRP inhibited the accumulation of phages expressing full-length peptide containing WRP (Table 2). Since PRPGAPLAGSWPGTS has a resembled sequence to WRP, namely PRP, we also focused on the PRP sequence and observed the inhibitory effect of the fragment peptide having N-terminus 8 mer, PRPGA-PLA, against the accumulation of PRPGA-PLAGSWPGTS-presented phage in tumors (Table 2). Based on these results, we modified liposomes with pentapeptides having PRP or WRP sequences and examined the biodistribution of these liposomes in tumor-bearing mice. All peptide-modified liposomes showed high accumulativeness in tumor tissue compared with control liposome (Figure 1a). In particular, APRPG-modified liposome (PRP-Lip) showed the highest accumulation in tumors. PRP-Lip had another feature, namely, it tends to avoid trapping by the reticuloendothelial system such as the spleen and liver (data not shown). Next, we examined the effect of APRPG incorporation into liposome on their *in vivo* behavior using positron emission tomography (PET). A PET study allows us to analyse real time distribution change of liposomes under non-invasive conditions. The time activity curves of liposomes indicated that PRP-Lip tended to accumulate in tumor time dependently (Figure 1b). This result was confirmed by the actual ^{18}F accumulation in the tumor, liver and spleen after PET scanning (data not shown).

Anti-neovascular therapy suppressed tumor growth

We then examined the suppression of tumor growth by the treatment of Meth A sarcoma-bearing mice with adriamycin (ADM), APRPG-modified liposome encapsulating ADM (PRP-LipADM), and control liposome

Table 1 Amino acid sequence of peptides presented in phages and their accumulation in tumor tissue

Amino acid sequence[a]	*Phage affinity against tumor*[c] *B16BL6 melanoma*	*Meth A sarcoma*
PRPGAPLAGSWPGTS (5)[b]	24.8	45.0
DR**WRP**ALPVVLFPLH	64.2	36.1
ASSSYPLIH**WRP**WAR	53.5	29.3
AAEWLDAFFVRHVDR	8.0	
GDVWLFLTSTSHFAR	5.2	
EGCSVSSVGALCTHV	4.8	
APCCSHLDASPFQRP	3.6	
PAQSNFVTWGYNVAV	2.8	
RASDVGSDVVPRYPF	1.5	

[a]The amino acid sequence designation is based on a single letter code. [b]The number of phage displaying the same peptide is indicated in parentheses. [c]Phage affinity was expressed as a fold of the control value obtained with random peptide expressing-phage accumulation

Table 2 Inhibitory effects of synthetic peptides against affinity-selected phage accumulation in tumor tissue

Phage-presented peptide	*Synthetic peptide*	*Inhibition (%)*
PRPGAPLAGSWPGTS	–	
	PRPGAPLAGSWPGTS	55
	ADGA**PRP**GAPLA	77
	GLDLLGDVRIPVVRR	0
DR**WRP**ALPVVLFPLH	–	
	DR**WRP**ALPVVLFPLH	66
	ASSSYPLIH**WRP**WAR	76
	DR**WRP**ALP	78
	GLDLLGDVRIPVVRR	0
ASSSYPLIH**WRP**WAR	–	
	DR**WRP**ALPVVLFPLH	43
	ASSSYPLIH**WRP**WAR	44
	IH**WRP**WAR	79
	GLDLLGDVRIPVVRR	0

[a]Inhibitory effect was determined as a reduction in percentage based on the control value obtained without the addition of synthetic peptide

encapsulating ADM (LipADM). Administration of PRP-LipADM suppressed the tumor growth most efficiently (Figure 2a). The superior effect of PRP-LipADM as compared to conventional LipADM may be explained by the increase of local concentration of ADM in tumor tissues. Alternatively, PRP-LipADM effectively damaged angiogenic endothelial cells that resulted in the indirect suppression of tumor growth. In general, liposomal anti-cancer drugs such as ADM are more efficient when the tumor growth reached several millimeters in diameter (Oku *et al*., 1994). It is because passive targeting or active targeting of liposomes to tumor tissues is well achieved, when tumors induce angiogenic vasculature. Thus, enhanced efficacy of liposomalization are depending on the schedule of treatment, PRP-LipADM might get more potent efficacy by optimizing that of treatment. The results also indicate that liposomalization itself is useful for decreasing side effects, since both PRP-LipADM and LipADM did not cause noticeable body weight change but free ADM-treated mice decreased in body weight progressively (data not shown). In fact, all free ADM-treated animals died of acute toxicity at a dose of 10 mg/kg (data not shown). Such reduction of the side effect was well known by liposomalization. The mean survival time for the control, LipADM-treated, and PRP-LipADM treated mice were 38.8, 47.7 and 50.2 days, respectively. PRP-LipADM was most efficient for prolonging survival time with an increased life span of about 30%. We also examined the suppression of tumor growth by PRP-LipADM in Colon 26 NL-17-bearing mice. PRP-LipADM also showed marked suppression against Colon 26 NL-17 (Figure 2b). The free ADM treatment group lost weight and three of six mice died of toxicity. The mean survival time for the control, LipADM-treated, and PRP-LipADM treated mice were 55.8, 69.7 and 72.3 days, respectively. Again, PRP-LipADM was the most efficient (about 30% increase in life span), and one of six mice was completely cured. We next examined the effect of PRP-LipADM on tumor-induced angiogenic vessels. As a result, PRP-LipADM markedly damaged newly forming blood vessels (Figure 2c). These results suggest that modification of liposome with APRPG enhanced the anti-tumor activity of ADM and reduced toxicity of ADM due to targeting effect. Furthermore, PRP-Lip has a possibility as a carrier of agents for anti-neovascular therapy, or to deliver anti-angiogenic agents to the angiogenic site.

Applicability of PRP-containing peptide to human

Finally we investigated whether the peptides selected in the murine angiogenic model have affinity for angiogenic endothelium in human tumors. Binding capacity of PRP-Lip and control liposome to human umbilical endothelial cells (HUVECs) was determined with con-focal microscope. NBD-labeled liposome bound to VEGF-activated HUVECs only when liposome was modified with APRPG (Figure 3a,b). This binding was cancelled in the presence of excess APRPG peptide (Figure 3c). The specific binding of PRP-Lip was not observed without stimulation of HUVECs with VEGF (Figure 3d). Furthermore, histochemical analysis demonstrated that biotinylated PRPGAPLAGSWPGTS specifically bound to angiogenic endothelial cells in human islet cell tumor of the pancreas and glioblastoma (Figure 4a,b). However, biotinylated peptide containing the WRP sequence, i.e., ASSSYPLIHWRPWAR, did not show the specific binding to endothelial cells in the islet cell tumor (data not shown). Pre-treatment with an excess of synthetic PRPGAPLAGSWPGTS inhibited the binding of biotinylated PRPGAPLAGSWPGTS in the glioblastoma tissue (Figure 4c). These data indicate that PRP-containing peptides have affinity to some molecule(s) on human angiogenic endothelial cells.

Discussion

In general, cancer chemotherapy is accompanied by strong side effects and acquired drug resistance. Therefore, drug delivery systems that selectively deliver the drugs to the target tumor are awaited. Many

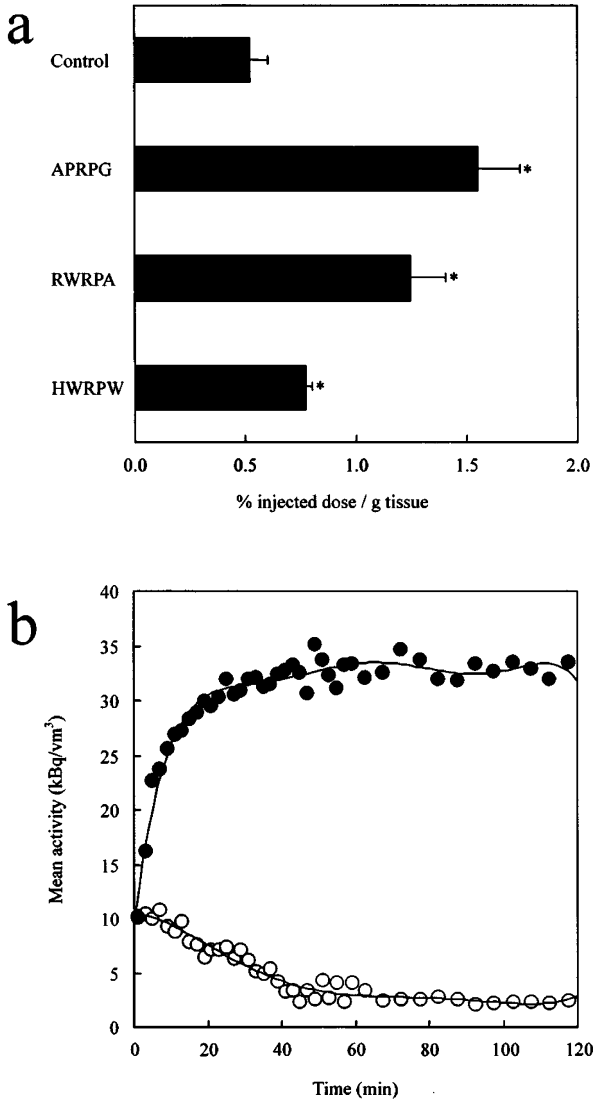

Figure 1 Accumulation of peptide-modified liposomes in the implanted tumor. (**a**) Traditional biodistribution study of various peptides-modified liposomes 3 h after injection revealed that APRPG-modified liposome most accumulated in the tumor, as compared with RWRPA-modified liposome, HWRPA-modified liposome, or control liposome in Meth A sarcoma-bearing mice. Data are presented as a per cent-injected dose per g tissue and s.d. Significant differences from the control are indicated ($*P<0.05$). (**b**) Real time accumulation change of APRPG-modified liposome and control liposome in tumor tissues demonstrated that the former liposome actively accumulated in tumor immediately after injection. This high accumulation was sustained for at least 120 min after injection during PET scanning

attempts have been made for this purpose including the usage of monoclonal antibodies against tumor tissues (Huang *et al*., 1997; Viti *et al*., 1999). Recently, vascular targeting has become a focus of interest, since certain drugs or drug carriers first meet neovasculature before extravasation in the tumor. Especially, targeting of a tumor angiogenic vasculature is promising for cancer treatment since these vessels have properties different from those of the preexisting systemic vasculature (Brower, 1999; Hanahan, 1997). Here, we revealed that angiogenic vasculature-specific peptides, PRPGAPLAGSWPGTS or APRPG, might be useful as tools for active targeting to tumor neovasculature.

Since we selected phage clones from DAS model mice instead of tumor-bearing mice, the selected amino acid sequences should be specific only for the angiogenic site but not for tumor tissues. Our results demonstrated that PRPGAPLAGSWPGTS-, DRWRPALPVVLFPLH-, and ASSSYPLIHWRPWAR-presented phage clones highly accumulated in two types of murine tumor. These data indicate that the homing capability of these phages was independent of tumor type, supporting the idea that they were not recognized by any tumor cell-surface molecule(s), but by some angiogenesis-related molecule(s). The amino acid sequences of these peptides have not been isolated in other screenings. There was no candidate molecule with significant homology to PRPGAPLAGSWPGTS and DRWRPALPVVLFPLH in a homology search, although the HWRPW sequence in ASSSYPLIHWRPWAR revealed to be identical to a part of the sequence of Flt-4, a receptor for VEGF-C. VEGF-C is known to bind to Flk-1/KDR as well as to Flt-4, and is reported to be an angiogenesis stimulator (Cao *et al*., 1998). The importance of the HWRPW sequence for the interaction of VEGF-C with its receptors, however, is not clear at present. The target molecule(s) of the novel peptides obtained here should be clarified in the future.

Liposomal homing study supports the idea that PRP and WRP sequences are important for the targeting to angiogenic sites, since two different particles carrying the sequence, namely, phage and liposomes, accumulated in tumor tissues, the former particle expressing the sequence, and the latter being modified by the sequence. Such small peptides are known to bind to certain specific proteins. For example, RGD-related peptides are known to interact with integrin $\alpha5\beta1$ and $\alpha v\beta3$. In fact, since the latter integrin is expressed on several tumor cells and angiogenic endothelium (Eliceiri and Cheresh, 1999), RGD-related peptides are reported to home in on the angiogenic endothelium of tumor-bearing mice after tail vein injection (Arap *et al*., 1998; Pasqualini *et al*., 1997).

Liposomes modified with pentapeptides having PRP or WRP showed high accumulativeness in the tumor. In particular, PRP-Lip showed the highest accumulation in the tumor. We also determined the biodistribution of liposomes modified with well-known peptides such as GRGDS and non-specific peptides such as LFPLH, and the accumulation of these liposomes in tumor tissues was observed to be less than that of APRPG-modified liposomes (data not shown). From the results of both biodistribution of liposomes and histochemical staining patterns of peptides, we decided to assess the effect of PRP-Lip as a drug carrier. We used 10 mol% peptide-containing liposome, because 5 or 10 mol% peptides-contained liposomes showed no significant differences in their biodistribution to 20 mol% peptide-modified liposomes (data not shown). Before *in vivo* therapeutic experiments, we determined

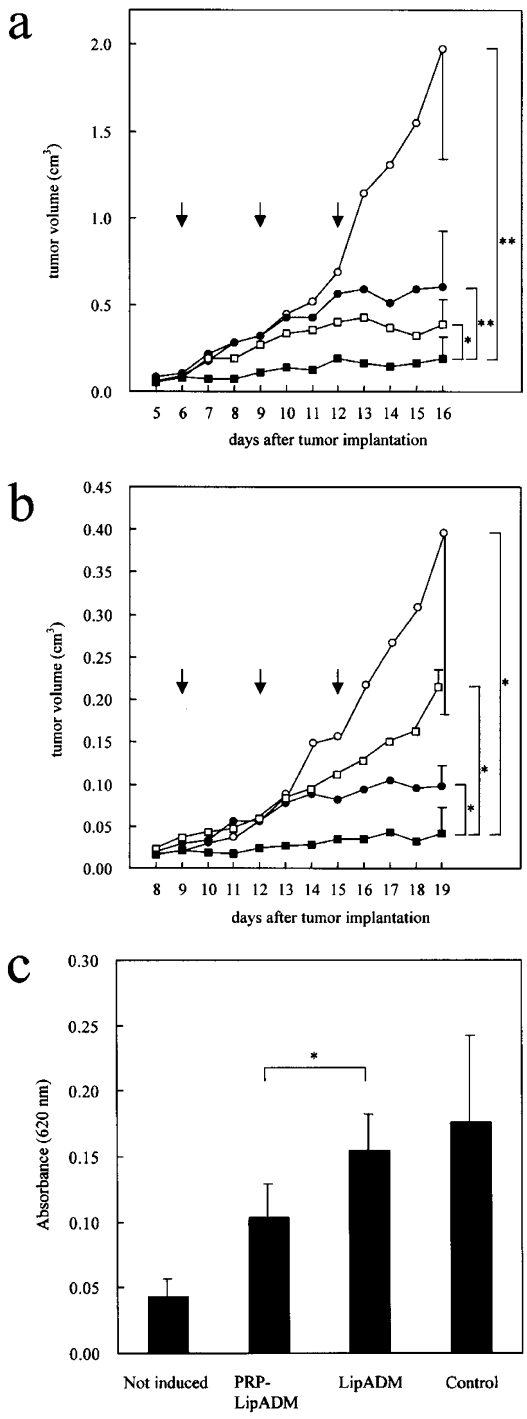

Figure 2 Suppression of tumor growth and angiogenesis *in vivo* by PRP-LipADM. (**a**,**b**) Tumor-bearing Balb/c mice were injected i.v. with 0.3 M glucose, ADM solution, LipADM, or PRP-LipADM. PRP-LipADM markedly suppressed tumor growth in Meth A sarcoma-bearing mice (**a**) ($n=6$; $^*P<0.05$; $^{**}P<0.01$) and in C26 NL-17-bearing mice (**b**) ($n=6$; $^*P<0.001$). Data is presented as mean tumor volume and s.d. Arrows show the day of treatment. (**c**) Suppression of *in vivo* angiogenesis by PRP-LipADM was significantly different from LipADM treatment ($n=4$-6; $^*P<0.05$) suggesting the anti-neovascular effect of PRP-LipADM. The relative amount of angiogenic vessels is indicated as Evans Blue accumulation at angiogenic site produced by DAS method and s.d.

the stability of LipADM and PRP-LipADM in the presence or absence of serum. These liposomes did not make aggregates in the presence of 50% serum. Furthermore, ADM release was not observed for at least 48 h from both liposomes in the presence of 50% serum, suggesting that these liposomes are quite stable during circulation *in vivo* (data not shown). These data suggest that peptide coating did not affect the physical properties of liposomes. In therapeutic experiments, modification of liposome with APRPG enhanced the anti-tumor activity of ADM and the reduced toxicity of it due to targeting effect. These effects of APRPG were independent of tumor type. Stability of PRP-LipADM suggests that these enhanced therapeutic efficacies did not cause the non-specific alteration of liposomes by peptide coating. The anti-tumor activity of PRP-LipADM may be explained partly by the increase of local concentration of ADM in the tumor. Although, we speculate that ADM damaged neovascular endothelial cells, since PRP-LipADM is expected to bind these growing cells efficiently from the results of both confocal observation and histochemical staining. However, further experiments are required for elucidating which factor is predominant between direct toxicity against tumor cells and indirect tumor growth suppression through toxic action against angiogenic endothelial cells. Taken together, it would be expected that PRP-Lip could deliver anticancer agents for anti-neovascular therapy, or anti-angiogenic agents for tumor dormancy therapy. Direct conjugation of the peptides with anticancer agents or angiogenesis inhibitors would also be possible for the purpose of anti-neovascular or anti-angiogenic therapy. Furthermore, it is considered that APRPG may be useful for human cancer treatment, since we demonstrated that PRP-Lip and PRPGAPLAGSWPGTS have affinity for VEGF-stimulated HUVECs and human tumor angiogenic endothelia, respectively.

Materials and methods

In vivo *biopanning and screening*

DAS model mice were prepared according to a modified method described previously (Kurohane *et al*., 2001). In brief, highly metastatic murine B16BL6 melanoma cells (1×10^7 cells/ring) were loaded into a Millipore chamber ring (Millipore Co., Bedford, MA, USA). The chamber rings were dorsally implanted into 5-week-old C57BL/6 male mice (Japan SLC Inc., Shizuoka, Japan). Five days after the implantation, these mice were used for *in vivo* biopanning.

A phage-displayed random peptide library expressing pentadecapeptides at the N terminus of pIII coat protein of M13 phage was kindly provided by Dr Hideyuki Saya of Kumamoto University (Nishi *et al*., 1996). *In vivo* biopanning was performed by a modified method as described by Pasqualini *et al*. (1997). In brief, 1.0×10^{13} colony-forming unit (c.f.u.) of the phage-displayed peptide library was injected into DAS model mice via a tail vein. Four minutes after injection, the phages that had accumulated in angiogenic vessels were recovered and titrated. Biopanning steps

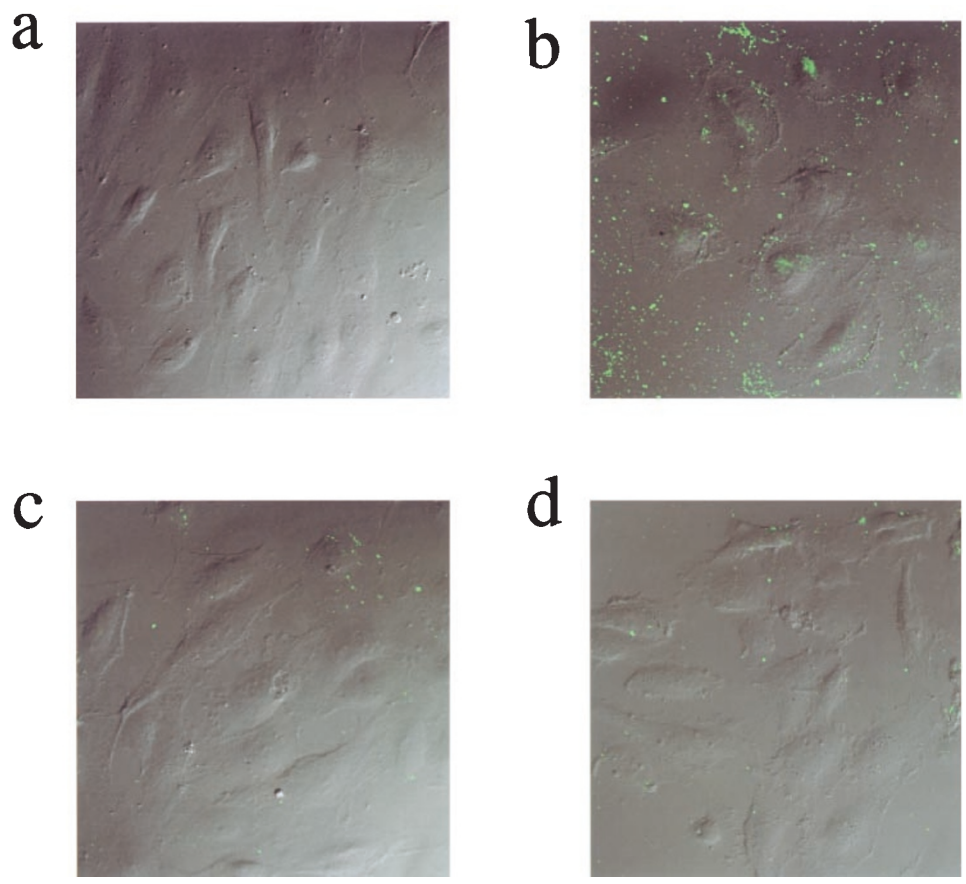

Figure 3 Specific binding of APRPG-modified liposome to VEGF-stimulated human umbilical endothelial cells. (**a**,**b**) Con-focal microscopic observation indicates the binding of PRP-Lip (**b**) to VEGF-stimulated HUVECs is specific in comparison with that of control liposome (**a**). (**c**) Moreover the binding of PRP-Lip was cancelled in the presence of excess APRPG, suggesting the presence of specific molecule(s) on the VEGF-stimulated HUVECs that have affinity to APRPG. (**d**) PRP-Lip did not bind to VEGF-unstimulated HUVECs

were repeated for five cycles. After selected phages were cloned, sequences of the peptides presented were determined as described previously (Ishikawa *et al*., 1998; Takikawa *et al*., 2000). For affinity screening, B16BL6 cells (1.0×10^6 cells/mouse) were implanted subcutaneously into the posterior flank of 5-week-old C57BL/6 male mice. Each sample of phage clones (1.0×10^{11} c.f.u.) was injected into tumor-bearing mice via a tail vein when the tumor size had become about 10 mm in diameter. Four minutes after injection, the phages that had accumulated in tumor tissue were recovered and titrated.

Peptides were synthesized using Rink amide resin (0.4–0.7 mmol/g) with the peptide synthesizer ACT357 (Advanced ChemTech). To examine the inhibitory effect of the synthetic peptide against phage accumulation, purified phage clone (5×10^8 c.f.u.) and 0.25 μmol of each synthetic peptide were co-injected into tumor-bearing mice. Four minutes after injection, the titer of phages recovered from the tumor tissue was determined.

Biodistribution study

Meth A sarcoma or Colon 26 NL-17 carcinoma cells (1.0×10^6 cells/mouse) were injected subcutaneously into the posterior flank of 5-week-old Balb/c male mice (Japan SLC Inc.), and biodistribution study was performed when the tumor size had become about 10 mm in diameter. Liposome composed of distearoylphosphatidylcholine (DSPC, gift from Nippon Fine Chemical Co. Ltd., Hyogo, Japan), cholesterol (Sigma, St. Louis, MO, USA), and stearoyl 5 mer peptide (APRPG, RWRPA or HWRPW), 10/5/2 as a molar ratio, was prepared, sized at 100-nm by extrusion through a pored filter, and radiolabeled with [oleate-1-^{14}C]cholesteryl-oleate (74 kBq/mouse, Amersham Pharmacia, Buckinghamshire, UK) as described previously (Oku *et al*., 1992). Size-matched Meth A sarcoma- or Colon 26 NL-17 carcinoma-bearing mice were injected with the radiolabeled liposomes via a tail vein. Three hours after the injection, the mice were sacrificed under diethyl ether anesthesia for the collection of the blood. After the mice had been bled from the carotid artery, the heart, lung, liver, spleen, kidney, and tumor were removed, washed with saline, and weighed. The radioactivity in each organ was determined with a liquid scintillation counter (Aloka, LSC-3500).

PET study

For positron emission tomography (PET) study, liposomes composed of DSPC: cholesterol = 2 : 1 (control liposome) or DSPC : cholesterol : stearoyl APRPG = 20 : 10 : 1 (PRP-Lip) as a molar ratio were prepared, sized at 100-nm, and loaded with [2-^{18}F]2-fluoro-2-deoxy-D-glucose. Then, liposomal traf-

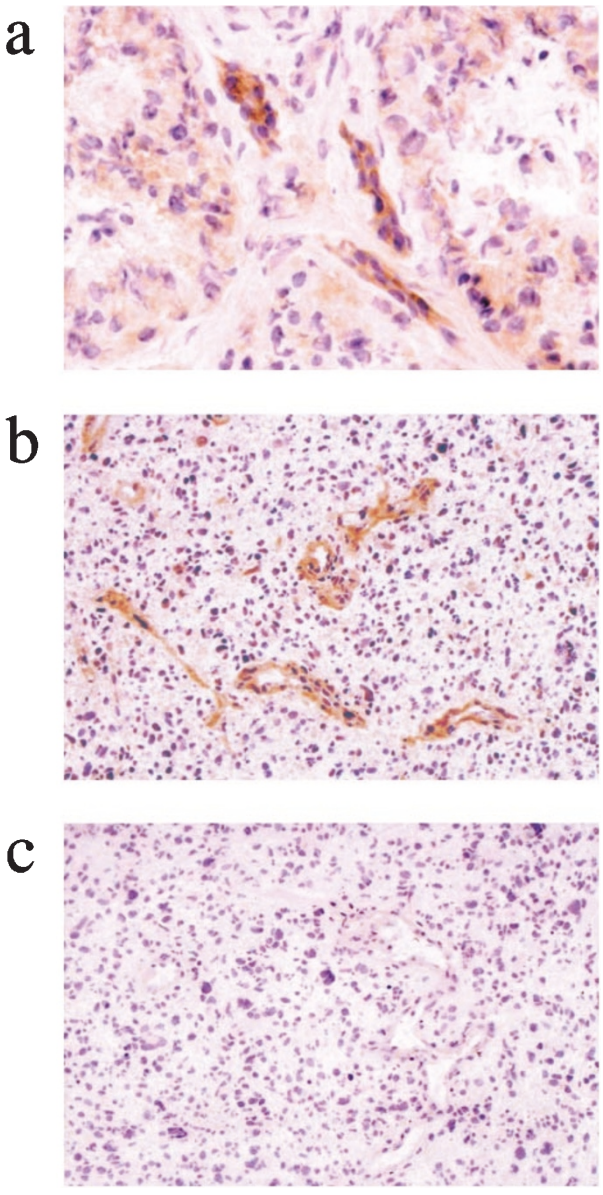

Figure 4 Specific binding of synthetic PRPGAPLAGSWPGTS to angiogenic vessels in human tumors. (**a**,**b**) Histochemical staining for biotinylated PRPGAPLAGSWPGTS depicted angiogenic vessels, indicating that PRPGAPLAGSWPGTS selectively bound to angiogenic endothelium in islet cell tumor of the pancreas (**a**) and in glioblastoma of the brain (**b**). (**c**) The specific staining pattern of biotinylated PRPGAPLAGSWPGTS in human glioma tissues was disrupted by pre-treatment of specimen with unlabeled PRPGAPLAGSWPGTS. Cell nuclei are counterstained with Mayer's hematoxylin

ficking in tumor bearing mice was analysed by PET as described previously (Asai *et al*., 1998; Oku, 1999b). In brief, Colon 26 NL-17 bearing Balb/c mice were anesthetized and injected via a tail vein with ^{18}F-labeled liposomes. The emission scan was started immediately after injection and performed for 120 min with an animal PET camera (Hamamatsu Photonics, SHR-7700). Time-activity curves were obtained from the mean pixel radioactivity in the region of interest (ROI) of the PET images. After the PET scan, the mice were sacrificed, and the biodistribution of ^{18}F was confirmed with a gamma-well scintillation counter.

Anti-tumor (anti-neovascular) activity of ADM-encapsulated neovasculature-homing liposome

Adriamycin (ADM)-encapsulated liposomes were prepared by a modification of the remote-loading method as described previously (Oku *et al*., 1994), and the encapsulation efficiency was more than 90% throughout the experiment. The liposomal size and composition were the same as the PET study. Tumor implantation was performed as described above. ADM-encapsulated in the control liposome (LipADM) or in liposome-modified with stearoyl APRPG (PRP-LipADM) (10 mg/kg as ADM), ADM alone (10 mg/kg), or 0.3 M glucose (control) were injected intravenously into tumor-bearing mice at days 6, 9 and 12 after implantation of Meth A sarcoma, or at days 9, 12 and 15 after implantation of Colon 26 NL-17 carcinoma cells. The sizes of the tumor and body weight of each mouse were monitored everyday. Tumor volume was calculated using the formula 0.4 ($a \times b^2$), where 'a' was the largest and 'b' was the smallest diameter of the tumor. Variance in a group was evaluated by the F-test, and differences in mean tumor volume were evaluated by Student's t-test.

For assay of anti-neovascular activity, a chamber ring loaded with Colon 26 NL-17 cells (1×10^7 cells/ring) was dorsally inoculated into Balb/c male mice. At 2 days after inoculation, LipADM, PRP-LipADM (10 mg/kg as ADM), ADM alone (10 mg/kg) or 0.3 M glucose were injected intravenously into DAS model mice. At 4 days after inoculation, 1% Evans Blue solution was injected intravenously into them. After 1 min, they were sacrificed and the pigment in the skin attached to the ring was extracted for the measurement of absorbance at 620 nm.

Confocal observation

NBD-phosphatidylethanolamine (NBD-PE)-labeled liposomes composed of DSPC: cholesterol: NBD-PE = 20 : 10 : 1 (control liposome) or DSPC : cholesterol : stearoyl APRPG : NBD-PE = 20 : 10 : 2 : 1 (PRP-Lip) as a molar ratio were prepared. HUVECs pre-treated with 100 ng/ml VEGF for 24 h were incubated with control liposomes or PRP-Lip for 30 min. To confirm the specific binding of PRP-Lip, HUVECs were incubated with PRP-Lip in the presence of 20-fold excess of free APRPG-peptides. HUVECs without stimulation of VEGF were also incubated with PRP-Lip. Then, HUVECs were washed with phosphate-buffered saline (PBS) and fixed with 2% paraformaldehyde – 0.2% glutaraldehyde in PBS. Localization of liposomes was monitored using LSM510 confocal system (Carl Zeiss Co., Ltd.).

Histochemical analysis

Biotinylated pentadecamer peptides were synthesized and used for histochemical analysis. Fresh tumor samples were obtained from patients with islet cell tumor of the pancreas or glioblastoma of the brain operated on Shinshu University Hospital, Matsumoto, Japan after informed consents were obtained. These samples were embedded in OCT compound, and frozen sections were fixed with 20% buffered formalin for 15 min. The formalin-fixed specimens were treated with 0.3% H_2O_2 in absolute methanol for 30 min. After washing, the specimens were incubated with 200 μg/ml biotinylated peptides solution in 4°C overnight and immersed in a horseradish peroxidase-labeled strep-

toavidin solution for 30 min. To determine the specificity of binding, adjacent sections of the specimens were incubated with excess synthetic peptides prior to the addition of biotinylated peptides. The peroxidase activity was developed in a diaminobenzidine-hydrogen peroxide solution. Cell nuclei were counterstained with Mayer's hematoxylin.

Acknowledgments
The authors thank Dr Yoji Ikawa at RIKEN for commenting on the manuscript. This work was supported in part by a Grant-in-Aid for Scientific Research from the Japan Society for the Promotion of Science and by Terumo Life Science Foundation. T Asai is a Research Fellow of the Japan Society for the Promotion of Science.

References

Asahara T, Murohara T, Sullivan A, Silver M, van der Zee R, Li T, Witzenbichler B, Schatteman G and Isner JM. (1997). *Science,* **275,** 964–967.

Asahara T, Takahashi T, Masuda H, Kalka C, Chen D, Iwaguro H, Inai Y, Silver M and Isner JM. (1999). *EMBO J.,* **18,** 3964–3972.

Asai T, Kurohane K, Shuto S, Awano H, Matsuda A, Tsukada H, Namba Y, Okada S and Oku N. (1998). *Biol. Pharm. Bull.,* **21,** 766–771.

Arap W, Pasqualini R and Ruoslahti E. (1998). *Science,* **279,** 377–380.

Boehm T, Folkman J, Browder T and O'Reilly MS. (1997). *Nature,* **390,** 404–407.

Browder T, Butterfield CE, Kraling BM, Shi B, Marshall B, O'Reilly MS and Folkman J. (2000). *Cancer Res.,* **60,** 1878–1886.

Brower V. (1999). *Nat Biotechnol.,* **17,** 963–968.

Brown JM and Giaccia AJ. (1998). *Cancer Res.,* **58,** 1408–1416.

Cao Y, Linden P, Farnebo J, Cao R, Eriksson A, Kumar, V, Qi JH, Claesson-Welsh L and Alitalo K. (1998). *Proc. Natl. Acad. Sci. USA,* **95,** 14389–14394.

Eliceiri BP and Cheresh DA. (1999). *J. Clin. Invest.,* **103,** 1227–1230.

Gho YS, Lee JE, Oh KS, Bae DG, and Chae CB. (1997). *Cancer Res.,* **57,** 3733–3740.

Hanahan D. (1997). *Science,* **277,** 48–50.

Healy JM, Murayama O, Maeda T, Yoshino K, Sekiguchi K and Kikuchi M. (1995). *Biochemistry,* **34,** 3948–3955.

Huang X, Molema G, King S, Watkins L, Edgington TS and Thorpe PE. (1997). *Science,* **275,** 547–550.

Ishikawa D, Kikkawa H, Ogino K, Hirabayashi Y, Oku N and Taki T. (1998). *FEBS Lett.,* **441,** 20–24.

Ito H, Rovira II, Bloom ML, Takeda K, Ferrans VJ, Quyyumi AA and Finkel T. (1999). *Cancer Res.,* **59,** 5875–5877.

Koivunen E, Gay DA and Ruoslahti E. (1993). *J. Biol. Chem.,* **268,** 20205–20210.

Kurohane K, Tominaga A, Sato K, North JR, Namba Y and Oku N. (2001). *Cancer Lett.,* **167,** 49–56.

Langer R. (1998). *Nature,* **392,** 5–10.

Martens CL, Cwirla SE, Lee RY, Whitehorn E, Chen EY, Bakker A, Martin EL, Wagstrom C, Gopalan P, Smith CW, Tate E, Koller KJ, Schatz PJ, Dower WJ and Barrett RW. (1995). *J. Biol. Chem.,* **270,** 21129–21136.

Nishi T, Budde RJA, McMurray JS, Obeyeskere NU, Safdar N, Levin VA and Saya H. (1996). *FEBS Lett.,* **399,** 237–240.

Oku N. (1999a). *Adv. Drug Deliv. Rev.,* **40,** 63–73.

Oku N. (1999b). *Adv. Drug Deliv. Rev.,* **37,** 53–61.

Oku N, Doi K, Namba Y and Okada S. (1994). *Int. J. Cancer,* **58,** 415–419.

Oku N, Namba Y and Okada S. (1992). *Biochim. Biophys. Acta,* **1126,** 255–260.

O'Reilly MS, Holmgren L, Chen C and Folkman J. (1996). *Nat. Med.,* **2,** 689–692.

Pasqualini R, Koivunen E and Ruoslahti E. (1997). *Nat. Biotechnol.,* **15,** 542–546.

Pasqualini R and Ruoslahti E. (1996). *Nature,* **380,** 364–366.

Scott JK and Smith GP. (1990). *Science,* **249,** 386–390.

Skobe M, Rockwell P, Goldstein N, Vosseler S and Fusenig NE. (1997). *Nat. Med.,* **3,** 1222–1227.

St Croix B, Rago C, Velculescu V, Traverso G, Romans KE, Montgomery E, Lal A, Riggins GJ, Lengauer C, Vogelstein B and Kinzler KW. (2000). *Science,* **289,** 1197–1202.

Takikawa M, Kikkawa H, Asai T, Yamaguchi N, Ishikawa D, Tanaka M, Ogino K, Taki T and Oku N. (2000). *FEBS Lett.,* **446,** 381–384.

Viti F, Tarli L, Giovannoni L, Zardi L and Neri D. (1999). *Cancer Res.,* **59,** 347–352.

Zetter BR. (1997). *Nat. Biotechnol.,* **15,** 1243–1244.